May 21st, 2020

Reaction Seminar

Dynamics and decay of three-body nuclei

Jesús Casal

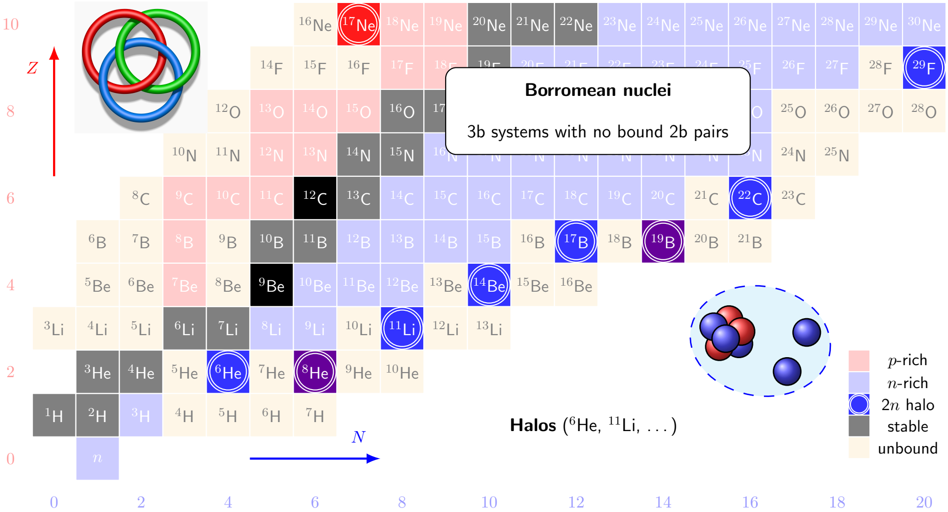
Borromean nuclei
3b systems with no bound 2b pairs
Halos (^{6}He, ^{11}Li, . . .)
p-rich
n-rich
$2n$ halo
stable
unbound
Z
N
10
8
6
4
2
0
0
2
4
6
8
10
12
14
16
18
20
^{16}Ne ^{17}Ne ^{18}Ne ^{19}Ne ^{20}Ne ^{21}Ne ^{22}Ne ^{23}Ne ^{24}Ne ^{25}Ne ^{26}Ne ^{27}Ne ^{28}Ne ^{29}Ne ^{30}Ne
^{14}F ^{15}F ^{16}F ^{17}F ^{26}F ^{27}F ^{28}F ^{29}F
^{12}O ^{13}O ^{14}O ^{15}O ^{16}O ^{25}O ^{26}O ^{27}O ^{28}O
^{10}N ^{11}N ^{12}N ^{13}N ^{14}N ^{15}N ^{24}N ^{25}N
^{8}C ^{9}C ^{10}C ^{11}C ^{12}C ^{13}C ^{14}C ^{15}C ^{16}C ^{17}C ^{18}C ^{19}C ^{20}C ^{21}C ^{22}C ^{23}C
^{6}B ^{7}B ^{8}B ^{9}B ^{10}B ^{11}B ^{12}B ^{13}B ^{14}B ^{15}B ^{16}B ^{17}B ^{18}B ^{19}B ^{20}B ^{21}B
^{5}Be ^{6}Be ^{7}Be ^{8}Be ^{9}Be ^{10}Be ^{11}Be ^{12}Be ^{13}Be ^{14}Be ^{15}Be ^{16}Be
^{3}Li ^{4}Li ^{5}Li ^{6}Li ^{7}Li ^{8}Li ^{9}Li ^{10}Li ^{11}Li ^{12}Li ^{13}Li
^{3}He ^{4}He ^{5}He ^{6}He ^{7}He ^{8}He ^{9}He ^{10}He
^{1}H ^{2}H ^{3}H ^{4}H ^{5}H ^{6}H ^{7}H
n

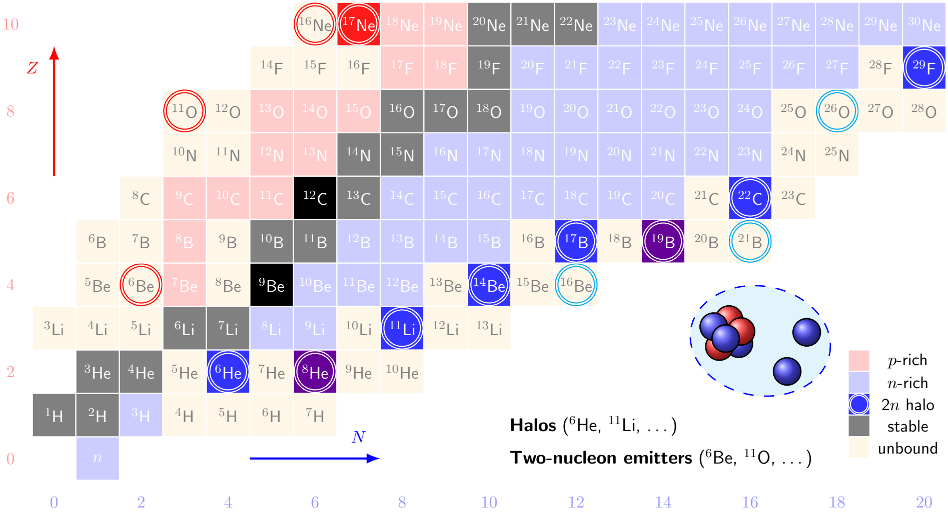

Halos (^{6}He, ^{11}Li, ...)

Two-nucleon emitters (^{6}Be, ^{11}O, ...)

1. Three-body hyperspherical harmonics (HH) formalism
   - Jacobi and hyperspherical coordinates
   - WF expansion and pseudostate method
2. Borromean two-neutron halo nuclei
   - Island of inversion
   - Possible halo and g.s. properties of ^{29}F
   - $E1$ response and Coulomb dissociation
3. Advanced reaction theory with three-body projectiles
   - Four-body CDCC (^{9}Be, ^{10}C)
4. Decay of three-body resonances
   - Resonance operator and identification in a discrete basis
   - Two-neutron emitters; nn relative energy spectrum
   - Application to ^{16}Be

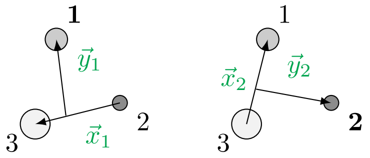

Jacobi coordinates

$\{x, y, \widehat{x}, \widehat{y}\}$

Hyperspherical coordinates

$\{\rho, \alpha, \widehat{x}, \widehat{y}\}$ $\quad \rho = \sqrt{x^2 + y^2} \quad \alpha = \arctan \frac{x}{y}$

$$\Psi^{j\mu}(\rho,\Omega) = \rho^{-5/2} \sum_{\beta} \chi_{\beta}^{j}(\rho) \mathcal{Y}_{\beta}^{j\mu}(\Omega) \qquad \beta \equiv \{K, l_x, l_y, l, S_x, J; I\}$$

Hyperspherical Harmonics (HH) expansion — hypermomentum $\widehat{K}$

$$\mathcal{Y}_{\beta}^{j\mu}(\Omega) = \left[\left(\Upsilon_{Klm_l}^{l_x l_y}(\Omega) \otimes \kappa_{S_x}\right)_J \otimes \phi_I\right]_{j\mu}$$

$$\Upsilon_{Klm_l}^{l_x l_y}(\Omega) = \varphi_K^{l_x l_y}(\alpha) \left[Y_{l_x}(\widehat{x}) \otimes Y_{l_y}(\widehat{y})\right]_{lm_l}$$

$$\varphi_K^{l_x l_y}(\alpha) = N_K^{l_x l_y} (\sin\alpha)^{l_x} (\cos\alpha)^{l_y} P_n^{l_x+\frac{1}{2}, l_y+\frac{1}{2}}(\cos 2\alpha)$$

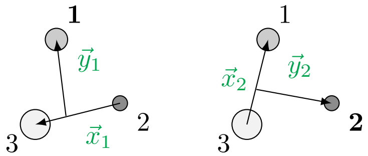

Jacobi coordinates $\{x, y, \widehat{x}, \widehat{y}\}$

Hyperspherical coordinates $\{\rho, \alpha, \widehat{x}, \widehat{y}\}$

$$\rho = \sqrt{x^2 + y^2} \qquad \alpha = \arctan\frac{x}{y}$$

$$\Psi^{j\mu}(\rho,\Omega) = \rho^{-5/2}\sum_{\beta}\chi_{\beta}^{j}(\rho)\mathcal{Y}_{\beta}^{j\mu}(\Omega) \qquad \beta \equiv \{K, l_x, l_y, l, S_x, J; I\}$$

Hyperspherical Harmonics (HH) expansion — hypermomentum $\widehat{K}$

$$\mathcal{Y}_{\beta}^{j\mu}(\Omega) = \left[\left(\Upsilon_{Klm_l}^{l_x l_y}(\Omega)\otimes\kappa_{S_x}\right)_J \otimes \phi_I\right]_{j\mu}$$

$$\Upsilon_{Klm_l}^{l_x l_y}(\Omega) = \varphi_K^{l_x l_y}(\alpha)\left[Y_{l_x}(\widehat{x})\otimes Y_{l_y}(\widehat{y})\right]_{lm_l}$$

$$\varphi_K^{l_x l_y}(\alpha) = N_K^{l_x l_y}\,(\sin\alpha)^{l_x}\,(\cos\alpha)^{l_y}\,P_n^{l_x+\frac{1}{2},l_y+\frac{1}{2}}\,(\cos 2\alpha)$$

Hyperradial functions are the solution of the coupled equations:

$$\left[-\frac{\hbar^2}{2m}\left(\frac{d^2}{d\rho^2}-\frac{15/4+K(K+4)}{\rho^2}\right)-\varepsilon\right]\chi_{\beta}^{j}(\rho)+\sum_{\beta'}V_{\beta'\beta}^{j\mu}(\rho)\chi_{\beta'}^{j}(\rho)=0$$

with coupling potentials $V_{\beta'\beta}^{j\mu}(\rho)$. Model space defined by **a given K_{max}**

$$V^{j\mu}_{\beta'\beta}(\rho) = \left\langle \mathcal{Y}^{j\mu}_{\beta}(\Omega) \middle| V_{12} + V_{13} + V_{23} \middle| \mathcal{Y}^{j\mu}_{\beta'}(\Omega) \right\rangle$$

- V_{ij} interaction between pairs

  central, spin-orbit, spin-spin, tensor. To reproduce binary subsystem

$$V^{j\mu}_{\beta'\beta}(\rho) = \left\langle \mathcal{Y}^{j\mu}_{\beta}(\Omega) \middle| V_{12} + V_{13} + V_{23} \middle| \mathcal{Y}^{j\mu}_{\beta'}(\Omega) \right\rangle + \delta_{\beta\beta'} V_{\mathsf{3b}}(\rho)$$

- V_{ij} interaction between pairs

  central, spin-orbit, spin-spin, tensor. To reproduce binary subsystem

- V_{3b} phenomenological three-body force

  diagonal term. Fixed to fine-tune the three-body energies

$$V_{\beta'\beta}^{j\mu}(\rho) = \left\langle \mathcal{Y}_{\beta}^{j\mu}(\Omega) \middle| V_{12} + V_{13} + V_{23} \middle| \mathcal{Y}_{\beta'}^{j\mu}(\Omega) \right\rangle + \delta_{\beta\beta'} V_{\mathsf{3b}}(\rho)$$

- V_{ij} interaction between pairs

  central, spin-orbit, spin-spin, tensor. To reproduce binary subsystem

- V_{3b} phenomenological three-body force

  diagonal term. Fixed to fine-tune the three-body energies

Pseudo-State (PS) method

$$\chi_{\beta}^{j}(\rho) = \sum_{i=0}^{N} C_{i\beta}^{j} U_{i\beta}(\rho)$$

expanded in $\mathcal{L}^2$ basis

N: number of hyperradial excitations included

$$\mathcal{H}\Psi_n^{j\mu} = \varepsilon_n \Psi_n^{j\mu}$$

- $\varepsilon_n < 0$ **bound states**
- $\varepsilon_n > 0$ **discretized continuum**

Analytical **T**ransformed **H**armonic **O**scillator **(THO)** basis

$$U_{i\beta}^{\mathrm{THO}}(\rho) = \sqrt{\frac{ds}{d\rho}} U_{iK}^{\mathrm{HO}}[s(\rho)]$$

$$s(\rho) = \frac{1}{\sqrt{2}\boldsymbol{b}} \left[\frac{1}{\left(\frac{1}{\rho}\right)^4 + \left(\frac{1}{\gamma\sqrt{\rho}}\right)^4} \right]^{\frac{1}{4}}$$

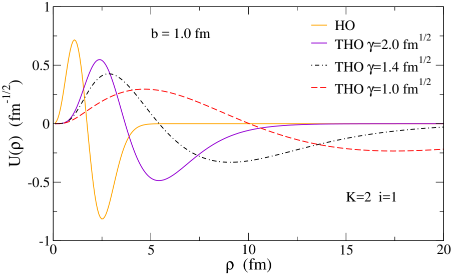

[PRC**88**(2013)014327]

Analytical **T**ransformed **H**armonic **O**scillator **(THO)** basis

$$U_{i\beta}^{\text{THO}}(\rho) = \sqrt{\frac{ds}{d\rho}} U_{iK}^{\text{HO}}[s(\rho)]$$

$$s(\rho) = \frac{1}{\sqrt{2}\boldsymbol{b}}\left[\frac{1}{\left(\frac{1}{\rho}\right)^4 + \left(\frac{1}{\gamma\sqrt{\rho}}\right)^4}\right]^{\frac{1}{4}}$$

Example:

$\Psi_n^{j\mu}(\rho,\Omega)$ PS spectra, ε_n
$b = 0.7$ fm

The ratio γ/b controls the density of PS as a function of the energy.

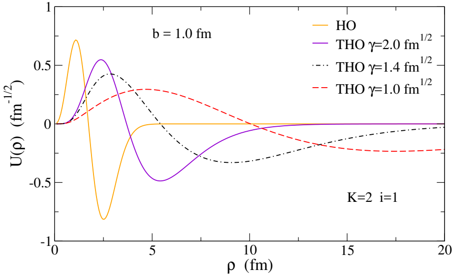

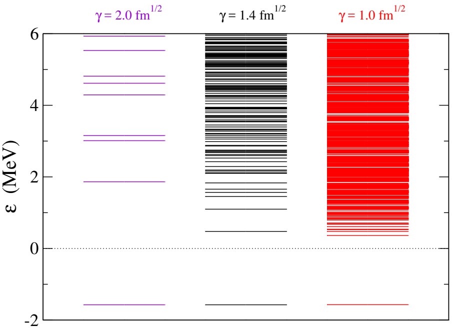

[PRC**88**(2013)014327]

Example: ^{9}Be photodissociation

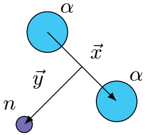

(α-α, α-n potentials fixed to ^{8}Be, ^{5}He)

$$\sigma_\gamma^{(\mathcal{O}\lambda)}(\varepsilon_\gamma) = \frac{(2\pi)^3(\lambda+1)}{\lambda[(2\lambda+1)!!]^2}\left(\frac{\varepsilon_\gamma}{\hbar c}\right)^{2\lambda-1}\frac{dB(\mathcal{O}\lambda)}{d\varepsilon}$$

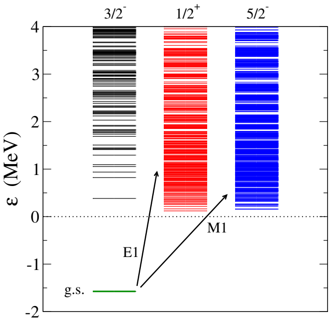

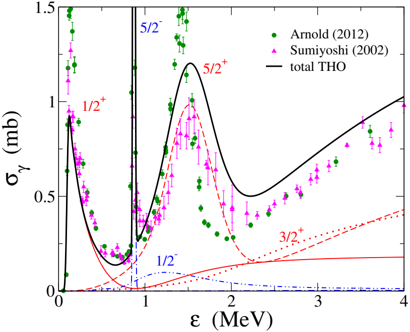

good description of resonant spectra [PRC**90**(2014)044304]

In a practical case:

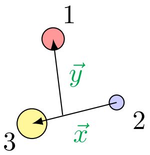

1. Choose (or fit) binary interactions V_{ij}
   Use exp. data if possible
   (e.g. phase shifts, two-body energies)
2. Diagonalize 3b Hamiltonian in a given basis
   (e.g. THO functions)
3. Ensure convergence of calculations, in particular for the g.s.
   K_{max}: size of the model space
   N: number of basis functions
   After covergence, possibly add three-body force $V_{3b}(\rho)$
4. Use PS to compute observables
   (e.g. $B(\mathcal{O}\lambda)$, ...)
   $\Rightarrow$ plug WF in reaction models to get cross sections

^{30}Al	^{31}Al	^{32}Al	^{33}Al	^{34}Al	^{35}Al	^{36}Al
^{29}Mg	^{30}Mg	^{31}Mg	^{32}Mg	^{33}Mg	^{34}Mg	^{35}Mg
^{28}Na	^{29}Na	^{30}Na	^{31}Na	^{32}Na	^{33}Na	^{34}Na
^{27}Ne	^{28}Ne	^{29}Ne	^{30}Ne	^{31}Ne	^{32}Ne	^{33}Ne
^{26}F	^{27}F	^{28}F	^{29}F	^{30}F	^{31}F	

$N = 20$

Island of inversion

Mg, Na, Ne isotopes around $N = 20$

Some degree of sd, pf *mixing*

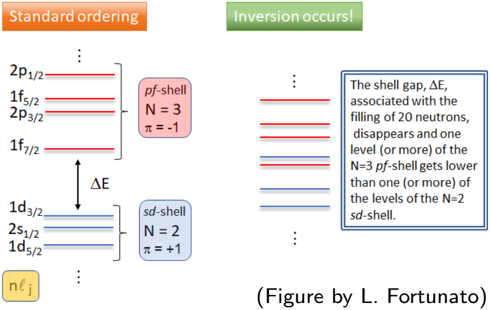

(Figure by L. Fortunato)

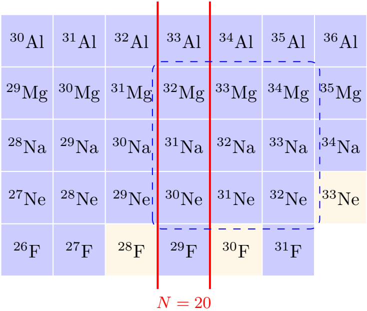

Island of inversion

Mg, Na, Ne isotopes around $N = 20$

Some degree of sd, pf mixing

$\Rightarrow$ F: southern shore of the island!

^{29}F is Borromean!
(^{27}F + n + n)
$\Rightarrow$ three-body model

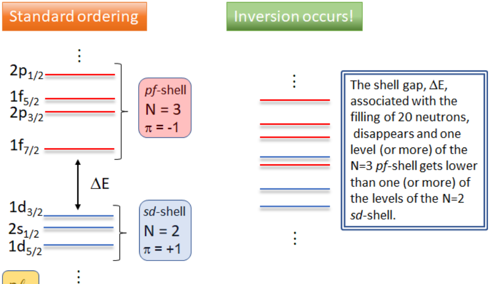

(Figure by L. Fortunato)

(the past)

Christian et al. (2012) ^{29}Ne($-1p$) on beryllium target

- PRL**108**(2012)032501
  Exploring the Low-Z Shore of the Island of Inversion at $N = 19$
- PRC**85**(2012)034327
  Spectroscopy of neutron-unbound ^{27,28}F

Invariant mass spectroscopy for ^{27}F + n

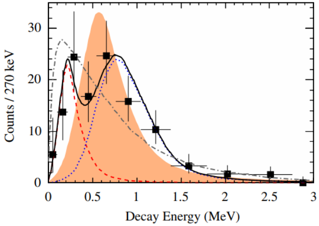

Two peaks (220, 810 keV)

"The measured ^{28}F ground state energy is in good agreement with USDA/USDB shell model predictions, indicating that pf shell intruder configurations play only a small role in the ground state structure of ^{28}F and establishing a low-Z boundary of the island of inversion for $N = 19$ isotones"

The NN interaction in ^{29}F brings the system back to a bound g.s.

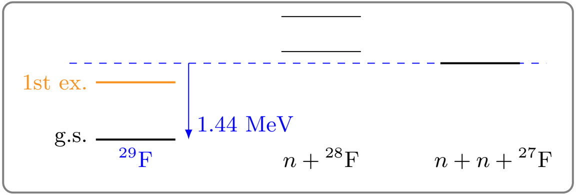

➢ $S_{2n}(^{29}\mathrm{F}) = 1.443(436)$ MeV; Gaudefroy et al. [PRL**109**(2012)202503]

The NN interaction in ^{29}F brings the system back to a bound g.s.

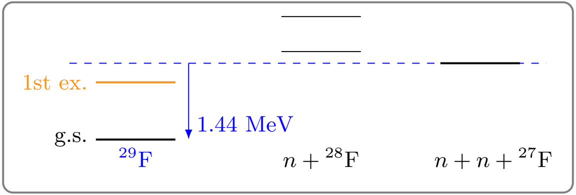

➢ $S_{2n}(^{29}\mathrm{F}) = 1.443(436)$ MeV; Gaudefroy et al. [PRL**109**(2012)202503]

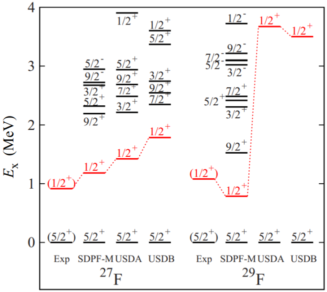

Excited state at $E_x = 1.080(18)$ MeV

Doornenbal et al. [PRC**95**(2017)041301]

SDPF shell-model calculations

"...indicate that the $N = 20$ gap is quenched for ^{29}F, thus extending the 'island of inversion' to isotopes with proton number $Z = 9$."

(the present)

Our work: three-body $(^{27}\text{F} + n + n)$ HH calculations for ^{29}F

➢ Need n-^{27}F interaction

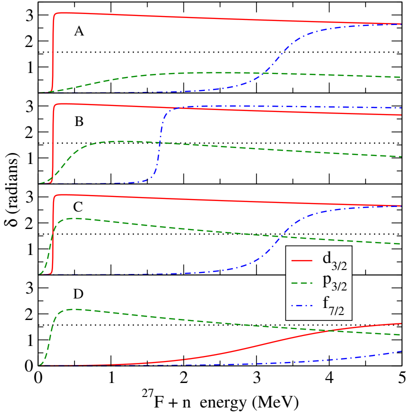

Inert core approx.

We consider different scenarios:

- A: standard shell-model
- B: intruder (low gap)
- C: degenerate
  $(1d_{3/2}$ and $2p_{3/2})$
- D: extremely inverted

(inspired by Christian's two-peak data)

Standard Woods-Saxon parametrization [PRC**102**(2020)24310]

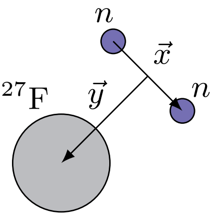

Solve the HH problem in the Jacobi T system

- core $+ n$ potentials A, B, C, D
- n-n interaction: GPT
  (tensor potential; PLB**32**(1970)591)

For simplicity, we ignore the spin of the core $\Rightarrow$ g.s. is 0^+
(possible core excitations effectively through ℓ-dependent potential)

Pauli states

Our core$+n$ potentials produce $1s_{1/2}$, $1p_{3/2}$, $1p_{1/2}$, $1d_{5/2}$ and $2s_{1/2}$ bound states which represent the fully occupied neutron orbitals of the core.

Removed using a supersymmetric transformation (phase equiv. potentials)

➢ In addition, (small) three-body force (Gaussian) to fix S_{2n}

Convergence of the ground state

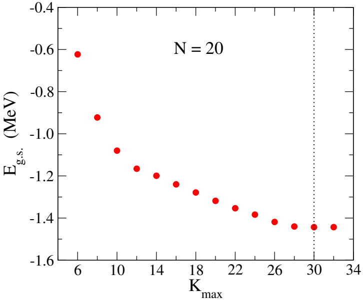

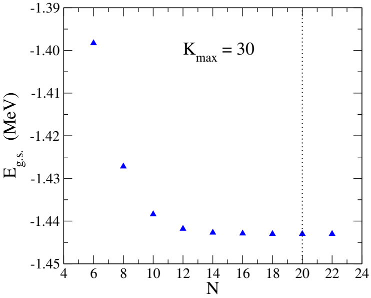

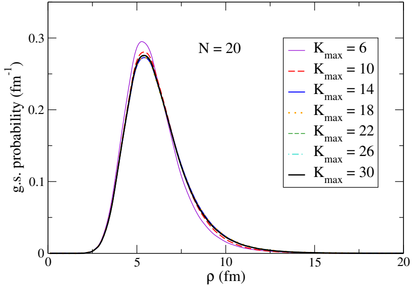

$K_{max} = 30$
$N = 20$

Wave function (and probability) well converged

(using set A: standard)

xy-probability:

$$\Psi_{g.s.}(\rho,\Omega) \to \Psi_{g.s.}(\boldsymbol{x},\boldsymbol{y})$$

dineutron and cigar-like
(set A: ratio close to 1)

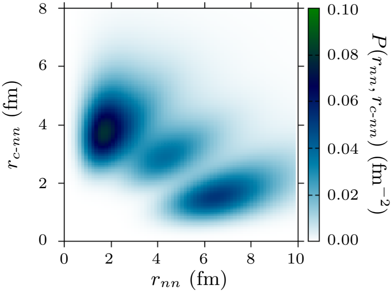

xy-probability:

$$\Psi_{g.s.}(\rho,\Omega) \rightarrow \Psi_{g.s.}(\boldsymbol{x},\boldsymbol{y})$$

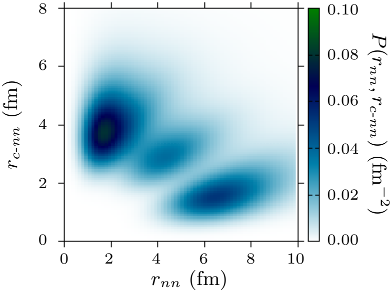

dineutron and cigar-like
(set A: ratio close to 1)

$(d_{3/2})^2$	$(f_{7/2})^2$	$(p_{3/2})^2$	R_m (fm)
81.3%	8.4%	6.8%	3.323

Rotation to **SM-like basis**:

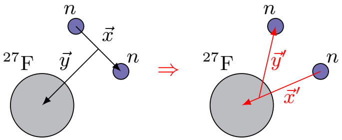

(Reynal-Revai coeff.)

small mixing with pf intruder

$\Delta R = R_m - R(^{27}\text{F}) = 0.105$ fm
little room for a $2n$ halo

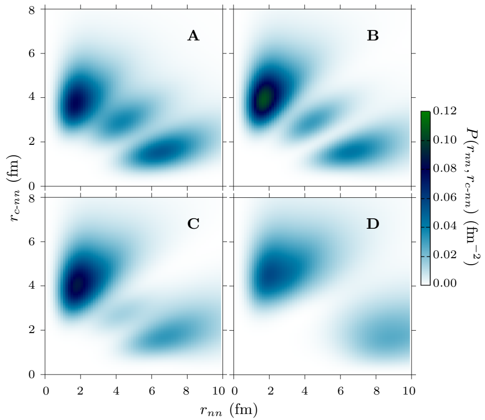

Dineutron enhancement with sets B and C (ratio $\sim$ 2)

Correlations due to mixing!

More details in:

Jagjit Singh, J. Casal, W. Horiuchi, L. Fortunato and A. Vitturi [PRC**100**(2020)024310]

%	$(d_{3/2})^2$	$(f_{7/2})^2$	$(p_{3/2})^2$	ΔR (fm)
A	81.3	8.4	6.8	0.105
B	50.7	21.1	21.6	0.129
C	45.4	7.4	39.8	0.162
D	4.2	2.1	85.4	0.241

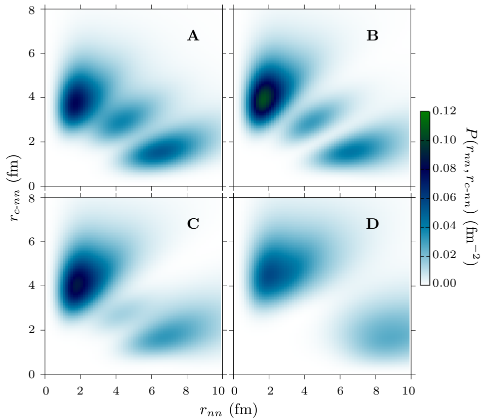

Dineutron enhancement with sets B and C (ratio ∼ 2)

Correlations due to mixing!

R_m increases with $(p_{3/2})^2$

ΔR values support moderate halo linked to parity inversion

(resembles ^{11}Li and its large s-wave intruder component)

More details in:

Jagjit Singh, J. Casal, W. Horiuchi, L. Fortunato and A. Vitturi [PRC**100**(2020)024310]

%	$(d_{3/2})^2$	$(f_{7/2})^2$	$(p_{3/2})^2$	ΔR (fm)
A	81.3	8.4	6.8	0.105
B	50.7	21.1	21.6	0.129
C	45.4	7.4	39.8	0.162
D	4.2	2.1	85.4	0.241

Recently... **new data arrived!** Revel et al. [PRL**124**(2020)152502]

a) ^{29}Ne$(-1p)$ and b) ^{29}F$(-1n)$ on a proton target

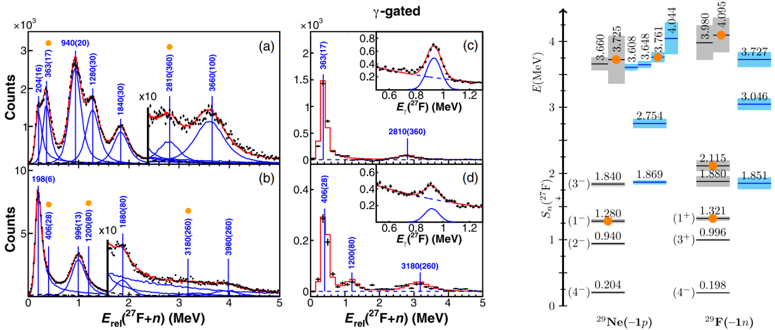

Recently. . . **new data arrived!** Revel et al. [PRL**124**(2020)152502]

a) ^{29}Ne$(-1p)$ and b) ^{29}F$(-1n)$ on a proton target

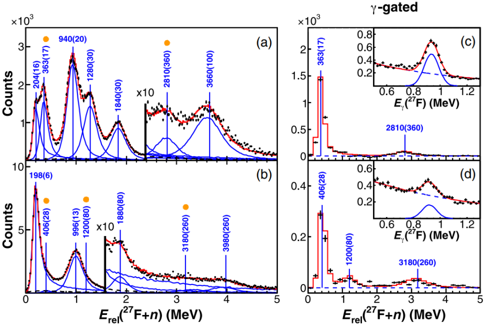

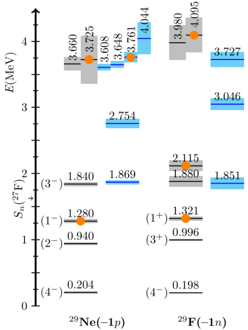

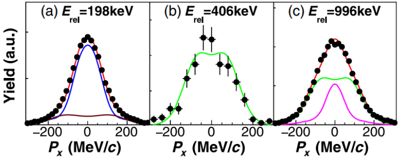

Momentum distributions:

g.s. $\ell = 1$ (79%) **inversion!**

1st $\ell = 2$ (72%)

(the future)

New potential set $D^\flat$: inverted, $2p_{3/2}$ and $1d_{3/2}$ fixed to Revel's data

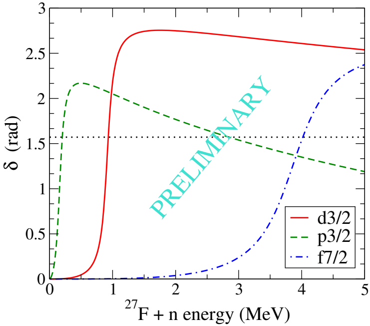

(the future)

New potential set $D^\flat$: inverted, $2p_{3/2}$ and $1d_{3/2}$ fixed to Revel's data

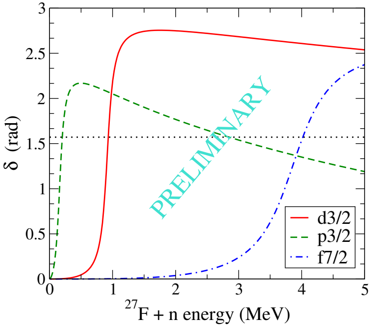

Repeat 3b calculations:

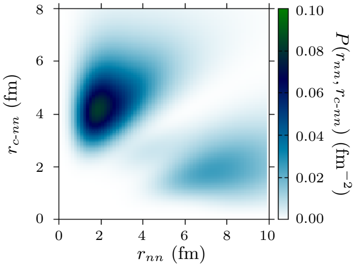

Mixing in ^{29}F:

$(d_{3/2})^2$	$(f_{7/2})^2$	$(p_{3/2})^2$	ΔR (fm)
28.1%	6.0%	57.5%	0.192

(the future)

New potential set $D^\flat$: inverted, $2p_{3/2}$ and $1d_{3/2}$ fixed to Revel's data

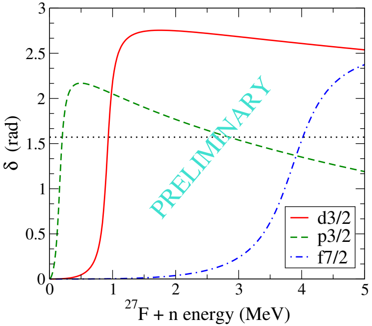

Repeat 3b calculations:

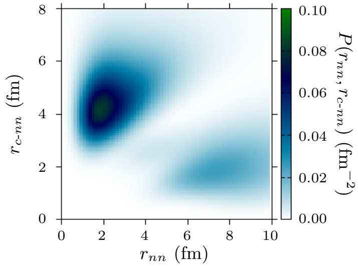

Mixing in ^{29}F:

$(d_{3/2})^2$	$(f_{7/2})^2$	$(p_{3/2})^2$	ΔR (fm)
28.1%	6.0%	57.5%	0.192

Strong dineutron component
Significant ΔR value

$\Rightarrow$ $2n$ halo in ^{29}F(g.s.)

Signature of halo in nuclear reactions?

- Large interaction cross sections [S. Bagchi et al., PRL (accepted)]
- Enhancement of low-energy electric dipole ($E1$) response

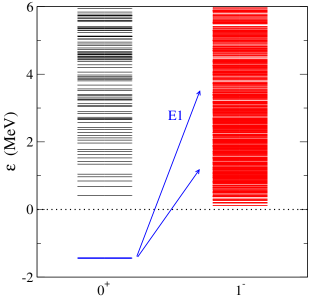

Signature of halo in nuclear reactions?

- Large interaction cross sections [S. Bagchi et al., PRL (accepted)]
- Enhancement of low-energy electric dipole ($E1$) response

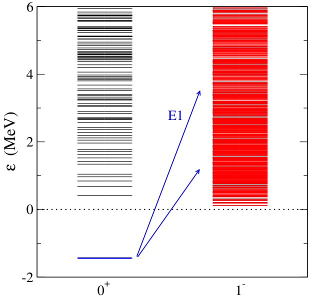

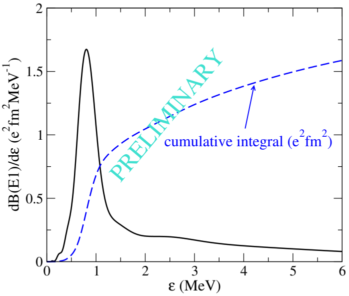

Signature of halo in nuclear reactions?

- Large interaction cross sections [S. Bagchi et al., PRL (accepted)]
- Enhancement of low-energy electric dipole ($E1$) response

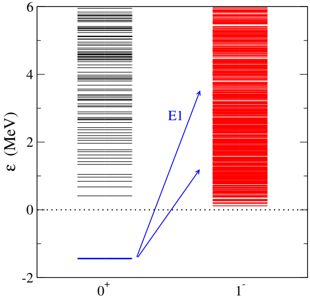

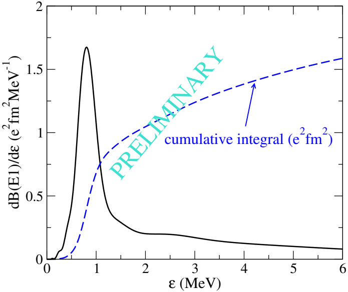

➢ Resonant state at $\sim$ 0.85 MeV: 73% of $(2p_{3/2})(1d_{3/2})$ components

E1 mostly $(2p_{3/2})^2 \rightarrow (2p_{3/2})(1d_{3/2})$ and $(1d_{3/2})^2 \rightarrow (2p_{3/2})(1d_{3/2})$

Signature of halo in nuclear reactions?

- Large interaction cross sections [S. Bagchi et al., PRL (accepted)]
- Enhancement of low-energy electric dipole ($E1$) response

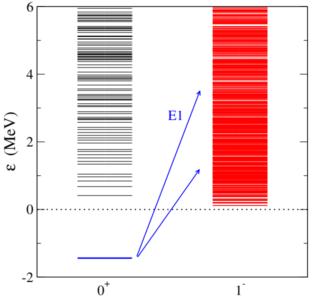

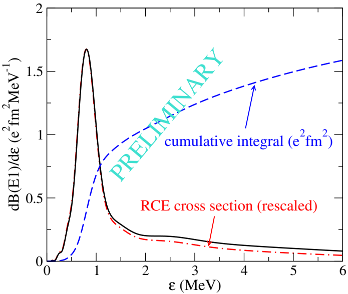

➢ Resonant state at $\sim$ 0.85 MeV: 73% of $(2p_{3/2})(1d_{3/2})$ components

E1 mostly $(2p_{3/2})^2 \rightarrow (2p_{3/2})(1d_{3/2})$ and $(1d_{3/2})^2 \rightarrow (2p_{3/2})(1d_{3/2})$

➢ Relativistic Coulomb Excitation (RCE) [A&W]

e.g. 235 MeV/nucleon ^{29}F beam on lead $\Rightarrow$ 600 mb (90% below 6 MeV)

What about low-energy breakup?

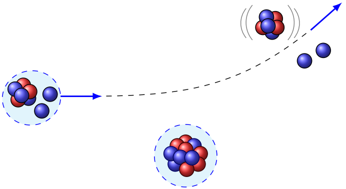

Around the Coulomb barrier, continuum couplings are essential in describing reactions involving weakly-bound nuclei

➢ need coupled channels (CC)

- Continuum-discretized coupled channels (CDCC)
  originally for deuteron breakup (Yahiro, Austern)

What about low-energy breakup?

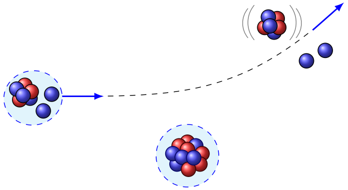

Around the Coulomb barrier, continuum couplings are essential in describing reactions involving weakly-bound nuclei

➢ need coupled channels (CC)

- Continuum-discretized coupled channels (CDCC) originally for deuteron breakup (Yahiro, Austern)

- Extended to three-body projectiles (e.g. ^{11}Li $+^{208}$ Pb M. Rodríguez-Gallardo et al)

[PRL**109**(2012)262701]

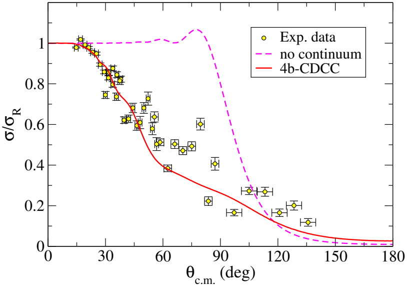

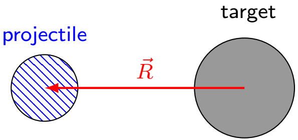

$$c \equiv \{L(nj)\}, \;\; \boldsymbol{J} = \boldsymbol{L} + \boldsymbol{j}$$

$$\Psi_c^{JM}(\boldsymbol{\xi}, \boldsymbol{R}) = \sum_{c'} \frac{i^L}{R} \chi_{c,c'}^J(R) \Phi_{c'}^{JM}(\widehat{R}, \boldsymbol{\xi})$$

$$\Phi_c^{JM}(\widehat{R}, \boldsymbol{\xi}) = \left[Y_L(\widehat{R}) \otimes \phi_{nj}(\boldsymbol{\xi}) \right]_{JM}$$

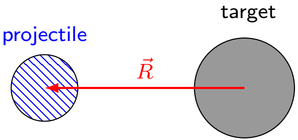

$$c \equiv \{L(nj)\}, \ \boldsymbol{J} = \boldsymbol{L} + \boldsymbol{j}$$

$$\Psi_c^{JM}(\boldsymbol{\xi}, \boldsymbol{R}) = \sum_{c'} \frac{i^L}{R} \chi_{c,c'}^J(R) \Phi_{c'}^{JM}(\widehat{R}, \boldsymbol{\xi})$$

$$\Phi_c^{JM}(\widehat{R}, \boldsymbol{\xi}) = \Big[Y_L(\widehat{R}) \otimes \phi_{nj}(\boldsymbol{\xi}) \Big]_{JM}$$

$$\left[-\frac{\hbar}{2m_r} \left(\frac{d^2}{dR^2} - \frac{L(L+1)}{R^2} \right) + E_{nj} - E \right] \chi_{c,c}^J(R) + \sum_{c'} i^{L'-L} V_{c,c'}^{JM}(R) \chi_{c,c'}^J(R) = 0$$

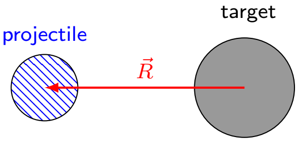

$$c \equiv \{L(nj)\}, \;\; \boldsymbol{J} = \boldsymbol{L} + \boldsymbol{j}$$

$$\Psi_c^{JM}(\boldsymbol{\xi}, \boldsymbol{R}) = \sum_{c'} \frac{i^L}{R} \chi_{c,c'}^{J}(R) \Phi_{c'}^{JM}(\widehat{R}, \boldsymbol{\xi})$$

$$\Phi_c^{JM}(\widehat{R}, \boldsymbol{\xi}) = \left[Y_L(\widehat{R}) \otimes \phi_{nj}(\boldsymbol{\xi}) \right]_{JM}$$

$$\left[-\frac{\hbar}{2m_r} \left(\frac{d^2}{dR^2} - \frac{L(L+1)}{R^2} \right) + E_{nj} - E \right] \chi_{c,c}^{J}(R) + \sum_{c'} i^{L'-L} V_{c,c'}^{JM}(R) \chi_{c,c'}^{J}(R) = 0$$

Requires $V_{c,c'}^{JM}(R) = \langle \Phi_c^{JM} | \widehat{U}_{pt} | \Phi_{c'}^{JM} \rangle$ coupling potentials;

typically expanded in Q multipoles

Three-body projectiles. 4-body CDCC

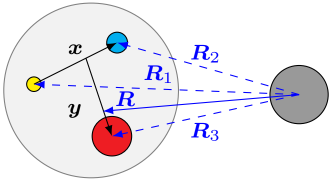

$$\widehat{U}_{pt} = U_1 + U_2 + U_3$$

$U_i \equiv$ optical potential between the particle i and the target

$\phi_{nj\mu}(\boldsymbol{x}, \boldsymbol{y})$ three-body states (HH)

Three-body projectiles. 4-body CDCC

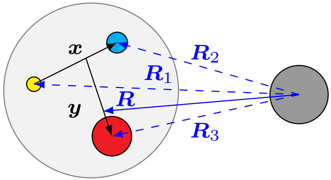

$\widehat{U}_{pt} = U_1 + U_2 + U_3$

$U_i \equiv$ optical potential between the particle i and the target

$\phi_{nj\mu}(\boldsymbol{x}, \boldsymbol{y})$ three-body states (HH)

1) binning method

$$h\phi_{j\mu}(\varepsilon) = \varepsilon\phi_{j\mu}(\varepsilon)$$

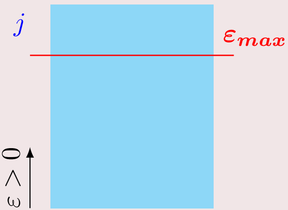

Three-body projectiles. 4-body CDCC

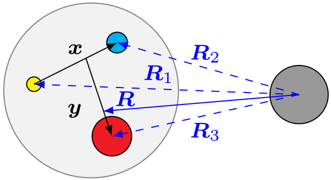

$\widehat{U}_{pt} = U_1 + U_2 + U_3$

U_i $\equiv$ optical potential between the particle i and the target

$\phi_{nj\mu}(\boldsymbol{x}, \boldsymbol{y})$ three-body states (HH)

1) binning method

$$h\phi_{j\mu}(\varepsilon) = \varepsilon\phi_{j\mu}(\varepsilon)$$

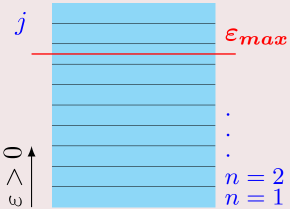

Three-body projectiles. 4-body CDCC

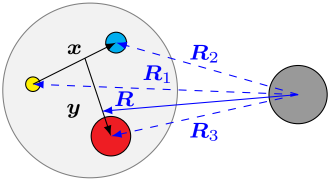

$$\widehat{U}_{pt} = U_1 + U_2 + U_3$$

$U_i \equiv$ optical potential between the particle i and the target

$\phi_{nj\mu}(\boldsymbol{x},\boldsymbol{y})$ three-body states (HH)

1) binning method

$$h\phi_{j\mu}(\varepsilon) = \varepsilon\phi_{j\mu}(\varepsilon)$$

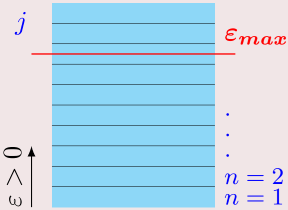

2) pseudostates (THO)

(useful for 3b systems with more than 1 charged particle)

Diagonalization:

$$h\phi_{nj\mu}(\varepsilon) = \varepsilon_n\phi_{nj\mu}(\varepsilon)$$

[PRC**92**(2015)054611]

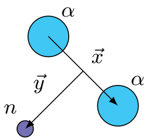

^{9}Be

$(\alpha + \alpha + n)$

weakly-bound

$\varepsilon_B = 1.574$ MeV

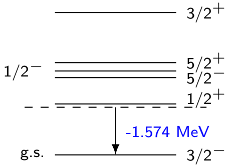

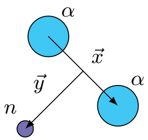

^{9}**Be**

$(\alpha + \alpha + n)$

weakly-bound

$\varepsilon_B = 1.574$ MeV

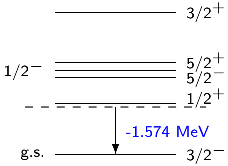

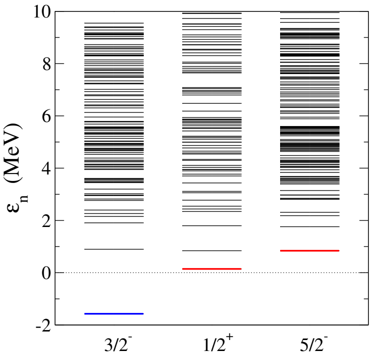

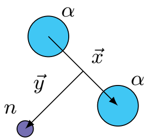

^{9}Be

$(\alpha + \alpha + n)$

weakly-bound

$\varepsilon_B = 1.574$ MeV

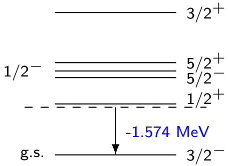

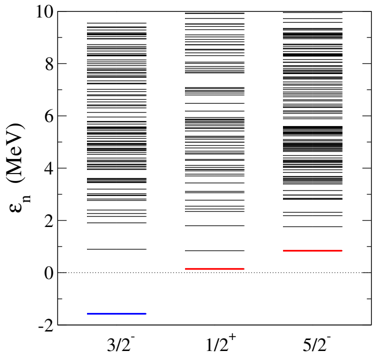

- $r_{mat} = 2.466$ fm
  (exp, 2.4-2.5 fm)
- $r_{ch} = 2.508$ fm
  (exp, 2.512 ± 0.012 fm)
- $Q_2 = 4.91$ e fm^2
  (exp, 5.29 ± 0.04 e fm^2)

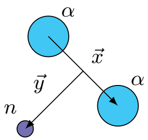

^{9}Be

$(\alpha + \alpha + n)$

weakly-bound

$\varepsilon_B = 1.574$ MeV

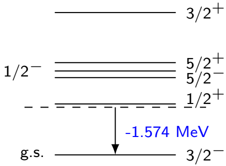

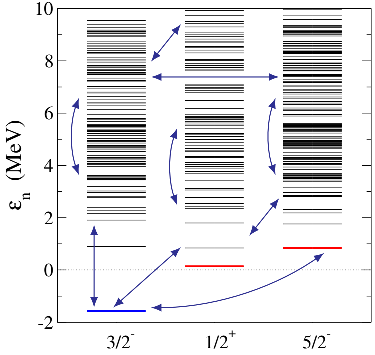

- $r_{mat} = 2.466$ fm
  (exp, 2.4-2.5 fm)
- $r_{ch} = 2.508$ fm
  (exp, 2.512 ± 0.012 fm)
- $Q_2 = 4.91$ e fm^2
  (exp, $5.29\pm$ 0.04 e fm^2)

CC: ground state, resonances and non-resonant continuum

^{9}Be + ^{208}Pb @ 44 MeV (around the Coulomb barrier)

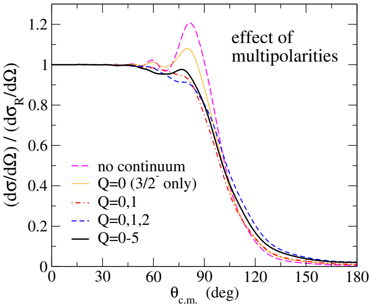

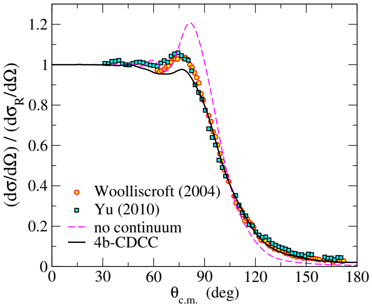

- Important dipole effects ($Q = 1$).
- Underestimation of the nuclear rainbow.
  (effect also observed by Descouvemont [PRC 2015])

  Hopefully breakup angular distributions will help!

^{9}Be + ^{208}Pb @ 38 MeV (below the barrier)

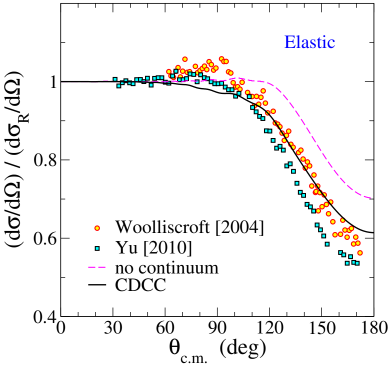

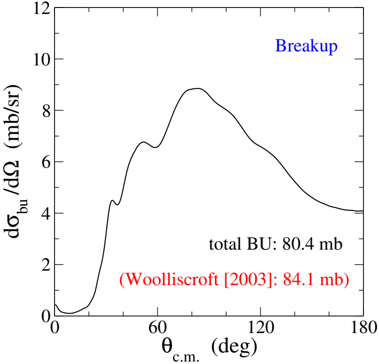

➢ Important continuum couplings even below the barrier.

➢ Agreement with data for total BU cross section.

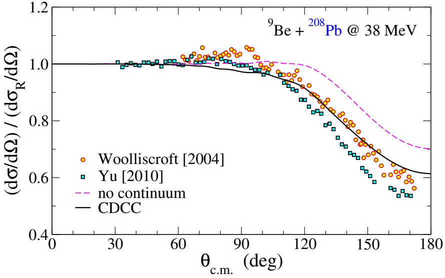

σ_{elas}, E_{lab} < Coulomb barrier

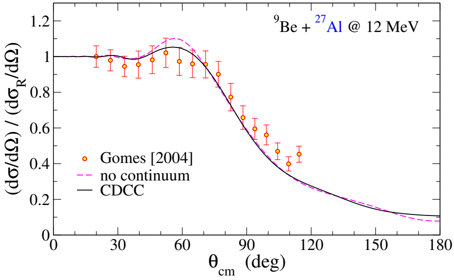

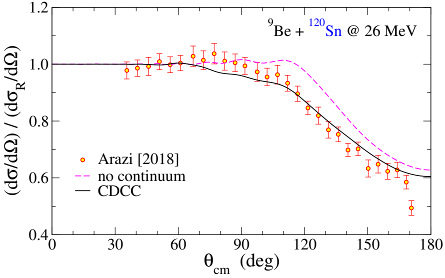

continuum effect decreases with Z

Coulomb breakup is important

PRC 92 (054611) 2015
PRC 97 (044607) 2018

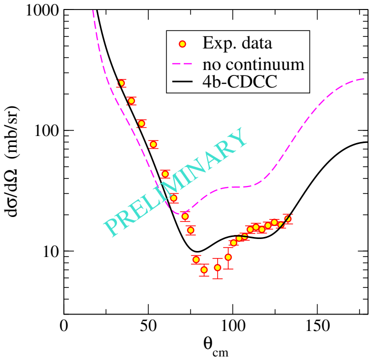

^{9}Be $+ p$ @ 51 MeV
(5.67 MeV/nucleon)

Data Keeley, Pakou et al. (2019)

Use n-p gaussian potential
and α-p OP by fitting elastic data

- ➢ The implicit inclusion of BU channels improves the agreement.
- ✗ Sensitivity to the potentials used; difficult to describe the minimum.

Other cases of interest and outlook

- ^{29}F(^{27}F $+ n + n$)

  Explore $2n$ halo dynamics around the barrier (compare ^{6}He or ^{11}Li)

- ^{17}Ne(^{15}O $+ p + p$)

  Is it a $2p$ halo? $\Rightarrow$ near-barrier dynamics could tell!

- ^{10}C is a Brunnian system

  ($\alpha + \alpha + p + p$ without any bound two- or three-body subsystem)

  Consider ^{8}Be $+ p + p$, with ^{8}Be in 0$^+$ g.s. (and possibly 2$^+$ ex)

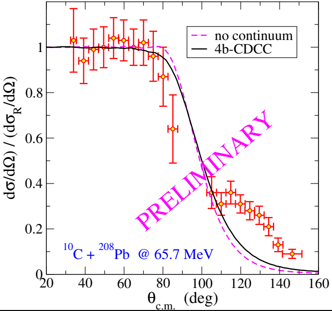

- *structure:*

  Need ^{8}Be $+ p$ potential

  Core excitation (2$^+$) ??

- *reaction:*

  Need ^{8}Be $+$ target OP

  (not well determined)

Data Linares et al. [to be submitted]
measured at Cyclotron Texas A&M

Other reactions: (p, pn) with Borromean projectiles (TC framework)

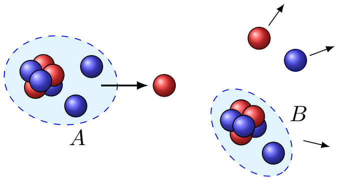

^{11}Li(p, pn) [PLB**772**(2017)115]

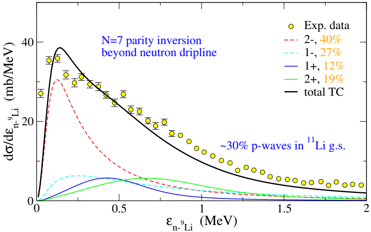

^{14}Be(p, pn) [PLB**797**(2019)134843]

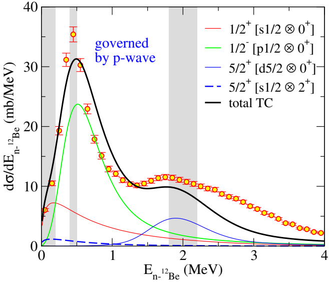

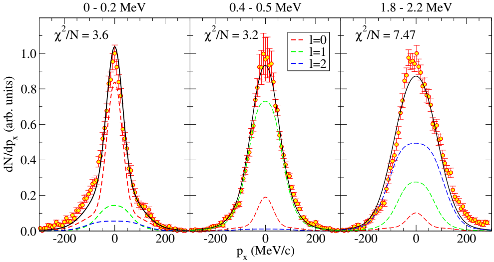

(seminars by M. Gómez-Ramos and A. Corsi)

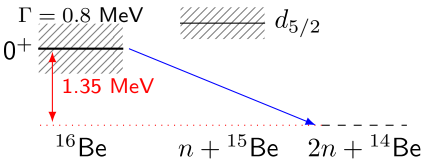

^{16}Be (^{14}Be $+ n + n$)

"Known" $2n$ emitter
Spyrou [PRL 108 (2012) 102501]

Proton removal from ^{17}B on Be target @ 53 MeV/u (MSU)

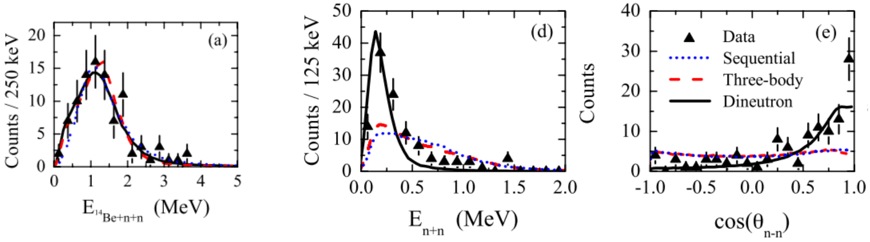

new RIKEN data - B. Monteagudo, F. M. Marqués (LPC Caen)

Three-body calculations

A. Lovell, F. M. Nunes and I. J. Thompson [PRC 95 (2017) 034605]

Hyperspherical R-matrix method ⇒ "true" continuum

- n-n GPT potential;
- n-^{14}Be potential fitted to g.s. of ^{15}Be ($d_{5/2}$) at 1.8 MeV

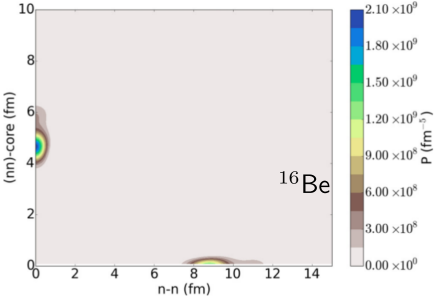

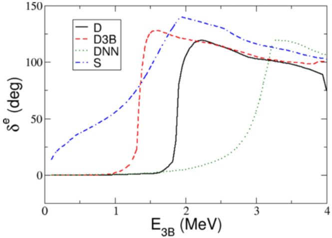

3b force to give 0^+ res. at $|S_{2n}| = 1.35$ ⇒ width $\Gamma = 0.17$ MeV

Dominant $2n$ configuration

80% $l_x = 0$ components

Stabilization approach by Hazi & Taylor PRA 1 (1970) 1109

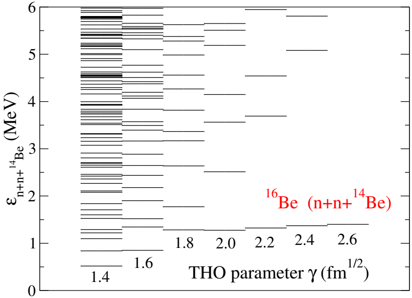

Stabilization in a discrete basis:

Look for stable pseudostates (PS) under changes in the basis parameters

⇒ PS around 1.3 MeV captures resonant behavior

J.C. [PRC **97** (2018) 034613]

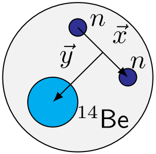

Dineutron dominates

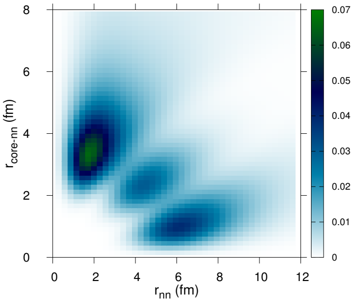

⇒ It favors correlated emission

Can we describe the decay?
(width, nn rel. energy, ...)

Identifying and characterizing few-body resonances: a novel approach

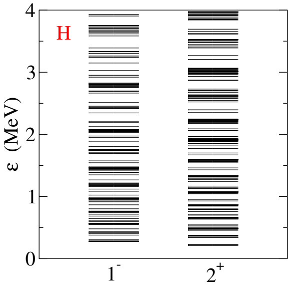

Ex: ^{6}He $(\alpha + n + n)$
non-res. 1^-
2^+ resonance

$\widehat{H}|n\rangle = \varepsilon_n|n\rangle$
mix res. and non-res.

[J.C., J. Gómez-Camacho, PRC **99** (2019) 014604]

Identifying and characterizing few-body resonances: a novel approach

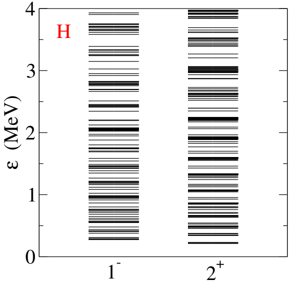

Ex: ^{6}He $(\alpha + n + n)$
non-res. 1^-
2^+ resonance

$\widehat{H}|n\rangle = \varepsilon_n|n\rangle$
mix res. and non-res.

$\Rightarrow$ Diagonalize a **resonance operator** in a PS basis $\{|n\rangle\}$

$$\widehat{M} = \widehat{H}^{-1/2}\widehat{V}\widehat{H}^{-1/2}, \qquad \widehat{M}|\psi\rangle = m|\psi\rangle; \qquad |\psi\rangle = \sum_n \mathcal{C}_n|n\rangle$$

- It separates resonant states, which are strongly localized, from non-resonant continuum states, which are spatially spread.
- The expansion in terms of $|n\rangle$ allows to build energy distributions.

[J.C., J. Gómez-Camacho, PRC **99** (2019) 014604]

Identifying and characterizing few-body resonances: a novel approach

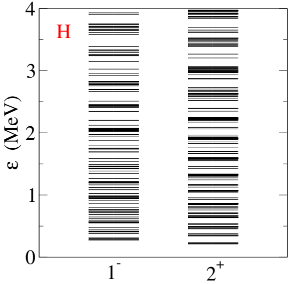

Ex: ^{6}He $(\alpha + n + n)$
non-res. 1^-
2^+ resonance

$\widehat{H}|n\rangle = \varepsilon_n|n\rangle$
mix res. and non-res.

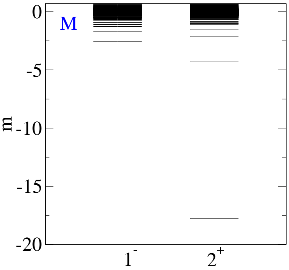

$\Rightarrow$ Diagonalize a **resonance operator** in a PS basis $\{|n\rangle\}$

$$\widehat{M} = \widehat{H}^{-1/2}\widehat{V}\widehat{H}^{-1/2}, \qquad \widehat{M}|\psi\rangle = m|\psi\rangle; \qquad |\psi\rangle = \sum_n \mathcal{C}_n|n\rangle$$

- It separates resonant states, which are strongly localized, from non-resonant continuum states, which are spatially spread.
- The expansion in terms of $|n\rangle$ allows to build energy distributions.

[J.C., J. Gómez-Camacho, PRC **99** (2019) 014604]

Decay ⇒ time evolution:

$$|\psi(t)\rangle = \sum_n \mathcal{C}_n e^{-i\varepsilon_n t}|n\rangle$$

Amplitudes:

$$a(t) = \langle\psi(0)|\psi(t)\rangle = \sum_n |\mathcal{C}_n|^2 e^{-i\varepsilon_n t}$$

Decay $\Rightarrow$ time evolution:

$$|\psi(t)\rangle = \sum_n \mathcal{C}_n e^{-i\varepsilon_n t}|n\rangle$$

Amplitudes:

$$a(t) = \langle\psi(0)|\psi(t)\rangle = \sum_n |\mathcal{C}_n|^2 e^{-i\varepsilon_n t}$$

For "ideal" BW:

$$a_r(t) = e^{-i\varepsilon_r t - \frac{\Gamma}{2}t}$$

Resonance quality parameter:

$$\delta^2(\varepsilon_r, \Gamma) = \frac{\int_0^\infty e^{-xt}|a(t) - a_r(t)|^2 dt}{\int_0^\infty e^{-xt}|a(t)|^2 dt}$$

($1/x$: relevant timescale for the resonance formation)

Decay ⇒ time evolution:

$$|\psi(t)\rangle = \sum_n \mathcal{C}_n e^{-i\varepsilon_n t}|n\rangle$$

Amplitudes:

$$a(t) = \langle\psi(0)|\psi(t)\rangle = \sum_n |\mathcal{C}_n|^2 e^{-i\varepsilon_n t}$$

For "ideal" BW:

$$a_r(t) = e^{-i\varepsilon_r t - \frac{\Gamma}{2}t}$$

Resonance quality parameter:

$$\delta^2(\varepsilon_r, \Gamma) = \frac{\int_0^\infty e^{-xt}|a(t) - a_r(t)|^2 dt}{\int_0^\infty e^{-xt}|a(t)|^2 dt}$$

($1/x$: relevant timescale for the resonance formation)

In order to find the resonance parameters ε_r and Γ which best describe the time evolution $a(t)$, we perform a minimization

$$\frac{\partial}{\partial\varepsilon_r}\delta^2(\varepsilon_r, \Gamma) = 0, \quad \frac{\partial}{\partial\Gamma}\delta^2(\varepsilon_r, \Gamma) = 0$$

⇒ as a function of x, i.e., $\varepsilon_r(x), \Gamma(x)$ $\quad$ $x \to 0$ limit means long times

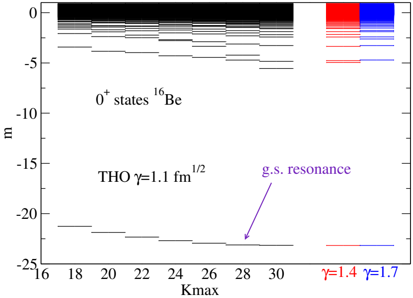

Resonance parameters

$\varepsilon_R(0^+) = 1.35$ MeV
$\Gamma(0^+) = 0.16$ MeV

width in good agreement with "true" 3b continuum (Lovell et al.)

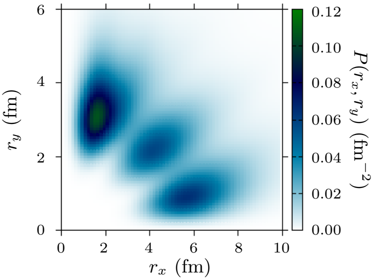

Resonance parameters

$\varepsilon_R(0^+) = 1.35$ MeV
$\Gamma(0^+) = 0.16$ MeV

width in good agreement with "true" 3b continuum (Lovell et al.)

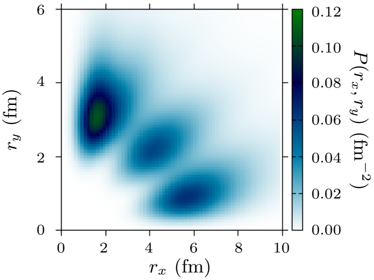

Resonance parameters

$\varepsilon_R(0^+) = 1.35$ MeV
$\Gamma(0^+) = 0.16$ MeV

width in good agreement with "true" 3b continuum (Lovell et al.)

We predicted also a 2^+ resonance

(no exp. yet)

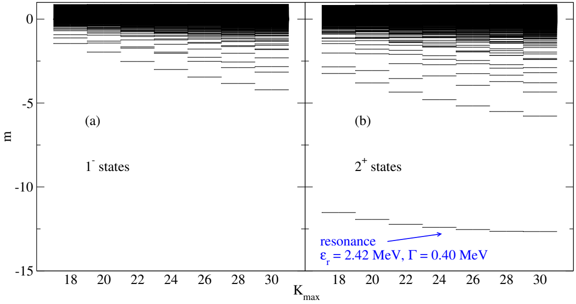

New RIKEN data resolve two peaks! (Monteagudo, Marqués)

1st excited state observed for the first time; likely 2^+

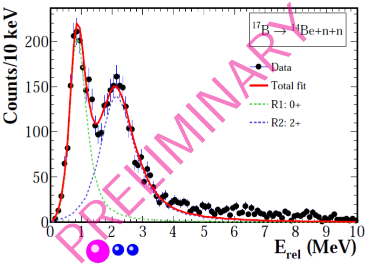

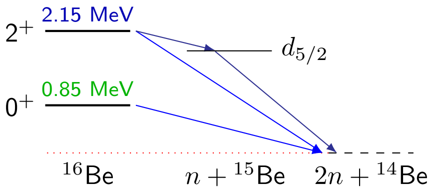

New RIKEN data resolve two peaks! (Monteagudo, Marqués)

1st excited state observed for the first time; likely 2^+

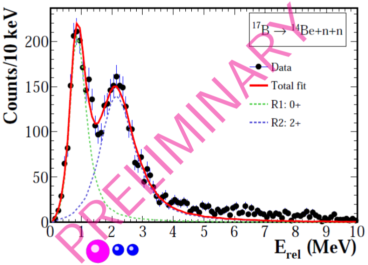

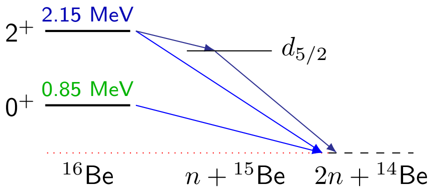

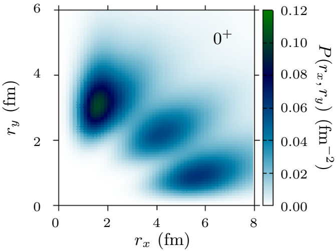

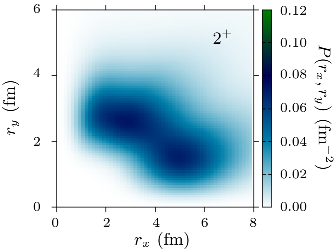

dineutron component is weak for the 2^+

Is there a signature of these dineutron correlations in the decay?

Resonance WF obtained as eigenstate of $\widehat{M}$, evolved in time:

$$\phi_\beta(\rho,t) \longrightarrow \left(\mathcal{A}_\beta^+ H_K^+(k_c\rho) + \mathcal{A}_\beta^- H_K^-(k_c\rho)\right) \exp(-\Gamma t/2 - iE_r t)$$

➢ Asymptotically, only outgoing waves $\mathcal{A}_\beta^+ H_K^+(k_c\rho)$ survive
This asymptotic behavior allows to build E_{nn} relative energy distributions

(in progress)

Is there a signature of these dineutron correlations in the decay?

Resonance WF obtained as eigenstate of $\widehat{M}$, evolved in time:

$$\phi_\beta(\rho,t) \longrightarrow \left(\mathcal{A}_\beta^+ H_K^+(k_c\rho) + \mathcal{A}_\beta^- H_K^-(k_c\rho)\right)\exp(-\Gamma t/2 - iE_r t)$$

➢ Asymptotically, only outgoing waves $\mathcal{A}_\beta^+ H_K^+(k_c\rho)$ survive
This asymptotic behavior allows to build E_{nn} relative energy distributions *(in progress)*

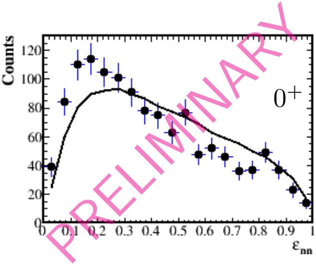

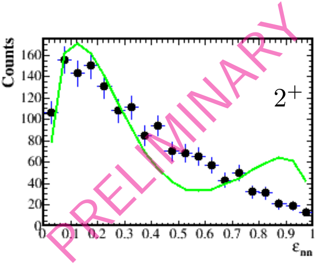

more pronounced low-E_{nn} peak for the 2^+!

Summary

- The structure and dynamics of **three-body nuclei** (e.g. Borromean, halos, $2N$-emitters) provide insight into the limits of nuclear stability: coupling to the continuum, parity inversion, exotic decays ...
- The hyperspherical harmonics (HH) formalism allows us to describe their properties. We use a pseudostate (PS) method [THO basis].

(1) Structure: possible $2n$ halo in ^{29}F (^{27}F $+ n + n$)

Data suggests ^{28}F g.s. is $\ell = 1$; inversion favors dineutron (mixing) and increases the radius of ^{29}F. We predict a large $E1$ strength.

(2) Reactions: four-body CDCC. ^{9}Be ($\alpha + \alpha + n$)

Coupling to the continuum is important even below the Coulomb barrier. Dipole effects are relevant.

(3) Decays: two-neutron emitter ^{16}Be (^{14}Be $+ n + n$)

Large dineutron component (favors simultaneous decay). The width obtained from the time evolution of the eigenstates of our resonant operator is consistent with "true" 3b continuum.

E_{nn} relative-energy dist. in progress (0^+, and 2^+ for the first time).

Summary

- The structure and dynamics of **three-body nuclei** (e.g. Borromean, halos, $2N$-emitters) provide insight into the limits of nuclear stability: coupling to the continuum, parity inversion, exotic decays . . .
- The hyperspherical harmonics (HH) formalism allows us to describe their properties. We use a pseudostate (PS) method [THO basis].

(1) Structure: possible $2n$ halo in ^{29}F (^{27}F $+ n + n$)

Data suggests ^{28}F g.s. is $\ell = 1$; inversion favors dineutron (mixing) and increases the radius of ^{29}F. We predict a large $E1$ strength.

(2) Reactions: four-body CDCC. ^{9}Be $(\alpha + \alpha + n)$

Coupling to the continuum is important even below the Coulomb barrier. Dipole effects are relevant.

(3) Decays: two-neutron emitter ^{16}Be (^{14}Be $+ n + n$)

Large dineutron component (favors simultaneous decay). The width obtained from the time evolution of the eigenstates of our resonant operator is consistent with "true" 3b continuum.

E_{nn} relative-energy dist. in progress (0^+, and 2^+ for the first time).

Summary

- The structure and dynamics of **three-body nuclei** (e.g. Borromean, halos, $2N$-emitters) provide insight into the limits of nuclear stability: coupling to the continuum, parity inversion, exotic decays ...
- The hyperspherical harmonics (HH) formalism allows us to describe their properties. We use a pseudostate (PS) method [THO basis].

(1) Structure: possible $2n$ halo in ^{29}F (^{27}F $+ n + n$)

Data suggests ^{28}F g.s. is $\ell = 1$; inversion favors dineutron (mixing) and increases the radius of ^{29}F. We predict a large $E1$ strength.

(2) Reactions: four-body CDCC. ^{9}Be ($\alpha + \alpha + n$)

Coupling to the continuum is important even below the Coulomb barrier. Dipole effects are relevant.

(3) Decays: two-neutron emitter ^{16}Be (^{14}Be $+ n + n$)

Large dineutron component (favors simultaneous decay). The width obtained from the time evolution of the eigenstates of our resonant operator is consistent with "true" 3b continuum.

E_{nn} relative-energy dist. in progress (0^+, and 2^+ for the first time).

Summary

- The structure and dynamics of **three-body nuclei** (e.g. Borromean, halos, $2N$-emitters) provide insight into the limits of nuclear stability: coupling to the continuum, parity inversion, exotic decays . . .
- The hyperspherical harmonics (HH) formalism allows us to describe their properties. We use a pseudostate (PS) method [THO basis].

(1) Structure: possible $2n$ halo in ^{29}F (^{27}F $+ n + n$)

Data suggests ^{28}F g.s. is $\ell = 1$; inversion favors dineutron (mixing) and increases the radius of ^{29}F. We predict a large $E1$ strength.

(2) Reactions: four-body CDCC. ^{9}Be ($\alpha + \alpha + n$)

Coupling to the continuum is important even below the Coulomb barrier. Dipole effects are relevant.

(3) Decays: two-neutron emitter ^{16}Be (^{14}Be $+ n + n$)

Large dineutron component (favors simultaneous decay). The width obtained from the time evolution of the eigenstates of our resonant operator is consistent with "true" 3b continuum.

E_{nn} relative-energy dist. in progress (0^+, and 2^+ for the first time).

Collaborators (theory):

J. M. Arias[1], L. Fortunato[2], J. Gómez-Camacho[1,3], M. Gómez-Ramos[4], W. Horiuchi[5], A. M. Moro[1], M. Rodríguez-Gallardo[1], Jagjit Singh[6], A. Vitturi[2]

Exp. colleagues: A. Arazi[7], A. Corsi[8], R. Linares[9], F. M. Marqués[10], B. Monteagudo[11]

[1]: Universidad de Sevilla, [2]: Università degli Studi di Padova and INFN, [3]: Centro Nacional de Aceleradores (CNA), [4]: TU Darmstadt, [5]: Hokkaido University, [6]: RCNP Osaka University, [7]: TANDAR, [8]: CEA Saclay, [9]: Universidade Federal Fluminense, [10]: LPC Caen [11]: MSU

FIS2017-88410-P

Horizon 2020
Grant agreement 654002

Project No.
CASA_SID19_1